

Hydration behaviour of synthetic saponite at variable relative humidity

KARMOUS MOHAMED SALAH* and JEAN LOUIS ROBERT†

Département de physique, faculté des sciences de Bizerte, 7021 Zarzouna, Tunisia

†IMPMC Campus Boucicaut, 140 rue de Lourmel, 75015 Paris, France

MS received 13 December 2010; revised 21 January 2011

Abstract. Hydration behaviour of synthetic saponite was examined by X-ray powder diffraction simulation at various relative humidities (RH). The basal spacing of the Ca-saponite increased stepwise with increase in RH. The (00 l) reflections observed reflect single or dual hydration states of smectite. Quasi-rational, intermediate, or asymmetrical reflections were observed for all XRD patterns and reflecting heterogeneity of the samples, especially along the transition between two hydration states.

Keywords. Hydration; saponite; XRD; simulation; RH.

1. Introduction

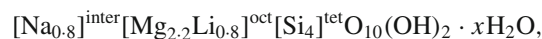
Smectites are 2:1 layered clays, each layer consisting of one sheet of octahedra between two sheets of silicon tetrahedra. Saponite is a trioctahedral smectites with all the octahedral positions occupied by divalent cations, generally Mg(II). Isomorphic substitutions with cations of lower oxidation state may occur in both sheets, producing a negatively charged layer, which is balanced by interlayer hydrated cations (Güven 1988; Karmous *et al* 2006, 2007). The moderate charge of the layers allows water molecules to penetrate the interlayer space and hydrate the interlayer cations, which results in a swelling of the crystal structure.

The swelling of smectites is complex (Laird 2006). The hydration of expandable 2:1 phyllosilicates has been extensively studied for over 50 years. Early work (Mooney *et al* 1952) demonstrated that smectite hydration is strongly influenced by H₂O vapour pressure (p/p_0), the extent of crystalline swelling, and the nature of the exchangeable cations. Recently, using XRD simulation, Karmous *et al* (2009) studied the influence of charge location on the hydration properties of synthetic saponite and hectorite under relative humidity, Ferrage *et al* (2010) demonstrated the hydration heterogeneity of different synthetic saponites with low and high charge and investigated about the ideal position of water molecule in the interlayer space.

This paper reports characterization of hydration properties of synthetic saponite exchanged with Ca cation.

2. Materials and methods

Synthetic saponite was prepared by hydrothermal synthesis in Morey-type externally heated pressure vessels (Karmous *et al* 2009). The started synthetic material has a structural formulae:



where x is the number of water molecules per cation.

The XRD analyses were carried out on a Brüker D8-advance using Cu-K α radiation. Data were recorded in the range of 5–35° 2 θ with a step of 0.02° 2 θ and a counting time of 80 s/step under controlled relative humidity (RH). Experimental XRD patterns were recorded at relative humidity (RH) conditions between 10% and ~90%. For each sample, XRD patterns were recorded following the same sequence of RHs, starting first from 35% (room) to 90% and then reducing RH down to 20% and 10%.

The mineralogical and structural characteristics were determined by comparing the experimental X-ray patterns with the theoretical patterns calculated from structural models (Pons *et al* 1995; Drits and Tchoubar 1990) and permits determination of the number and position of the intercalated water molecules. XRD patterns were calculated using the z -coordinates, where the origin of the atomic coordinates was taken at the basal oxygen atoms (Karmous *et al* 2009). The diffracted intensity for a unit-cell along the 00 rod of the reciprocal space is given by the following expression developed by Ben Haj Amara *et al* (1998):

$$I_{00}(2\theta) = L_p \text{Spur} \left(\text{Re}[\phi][W] \left\{ [I] + 2 \sum_n^{M-1} [(M-n)/M][Q]^n \right\} \right), \quad (1)$$

*Author for correspondence (karmoussalah@yahoo.fr)

with $L_p = \psi \frac{1 + \cos^2 2\theta}{\sin 2\theta}$, where Ψ is the orientation factor of the particles, Re the real part of the final matrix, Spur , the sum of the diagonal terms of the real matrix; M , the number of layers per stack; n , an integer varying between 1 and $M - 1$; $[\Phi]$, the structure factor matrix $[I]$, the unit matrix $[W]$, the diagonal matrix of the proportions of the different kinds of layers, and $[Q]$ the matrix representing the interference phenomena between adjacent layers. For a system made up of two types of layers (A and B) and a nearest neighbour interaction, $[Q]$ takes the form

$$\det Q = \begin{vmatrix} P_{AA}\exp(-2i\pi s d_A) & P_{AB}\exp(-2i\pi s d_A) \\ P_{BA}\exp(-2i\pi s d_B) & P_{BB}\exp(-2i\pi s d_B) \end{vmatrix}, \quad (2)$$

where s is the modulus of the scattering vector; $s = \frac{2 \sin \theta}{\lambda}$, d_A and d_B are the d -spacing of layers A and B , respectively and P_{AB} the conditional probability of passing from layer A to layer B . The relationship between different kinds of layer proportions and probabilities are given by

$$W_A + W_B = 1, \quad P_{AA} + P_{AB} = 1, \quad P_{BA} + P_{BB} = 1$$

and $W_A P_{AB} = W_B P_{BA}$.

The overall fit quality was assessed using the unweighted R_p parameter (Howard and Preston 1989)

$$R_p = \sqrt{\frac{\sum [I_{\text{obs}}(2\theta_i) - I_{\text{calc}}(2\theta_i)]^2}{\sum I_{\text{obs}}(2\theta_i)^2}}, \quad (3)$$

where I_{obs} and I_{calc} represent, respectively measured and calculated intensities, at position $2\theta_i$, the subscript i running over all points in the refined angular range. This parameter is mainly influenced by the most intense diffraction maxima, such as the $00l$ reflection, which contains essential information on the proportions of the different layer types and on their layer thickness.

The structural characteristics along the normal to the layer plane (z) were determined by comparing the experimental X-ray patterns with theoretical ones calculated from structural models; by fitting positions and profiles of the $00l$ reflections over a large angular range, the relative proportions of the different layer types can be determined together with the thickness and water content of the different layer types (Karmous *et al* 2009).

3. Results and discussion

The hydration state of smectites has been described using four layer types of different layer thicknesses and corresponding to the most common hydration states reported for smectites in non-saturated conditions: dehydrated layers (0 W, layer thickness ~ 9.6 – 10.1 Å), monohydrated layers (1 W, layer thickness ~ 12.3 – 12.7 Å), and bi-hydrated layers (2 W, layer thickness ~ 15.1 – 15.8 Å) and trihydrated (3 W, layer thickness ~ 18 – 19 Å) layers, the latter being less common (Ferrage *et al* 2005a,b). However, it was soon recognized that different hydration states/layer types usually coexist even under controlled conditions due to structural heterogeneities affecting the layer charge distribution (from one interlayer to the other or within a given interlayer) and/or location. Such a coexistence is for instance revealed by the irrationality of the $00l$ reflection series and by peak profile asymmetry at the transition between two hydration states (Karmous *et al* 2009).

The XRD patterns of Ca saponite recorded at relative humidity between 20 and 80% are shown in figure 1. The qualitative study shows that it is characterized by asymmetrical $00l$ reflections and a d_{001} spacing of 12.91 to 13.58 Å for RH rates $\leq 40\%$ (figures 1a and b), this corresponds to heterogeneous hydration state with different layer types (1 W and 2 W). At 60% RH, the $00l$ reflection is at 15.74 Å indicating

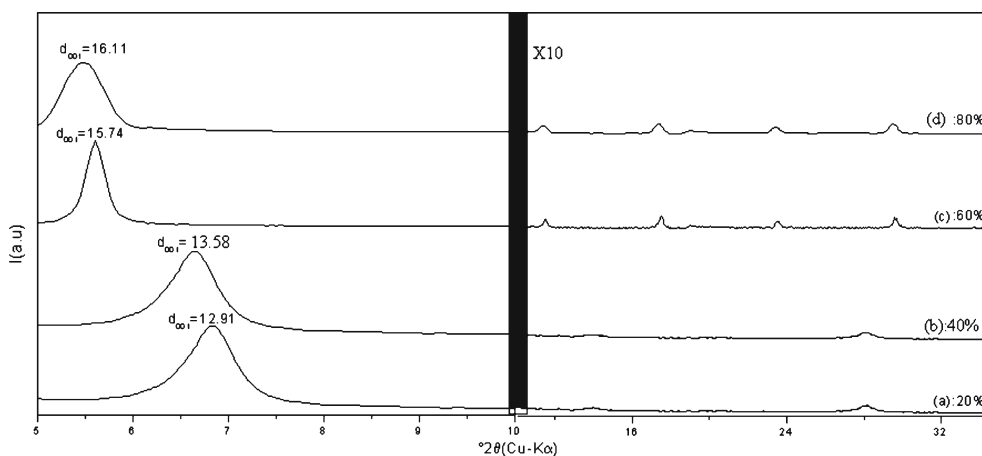
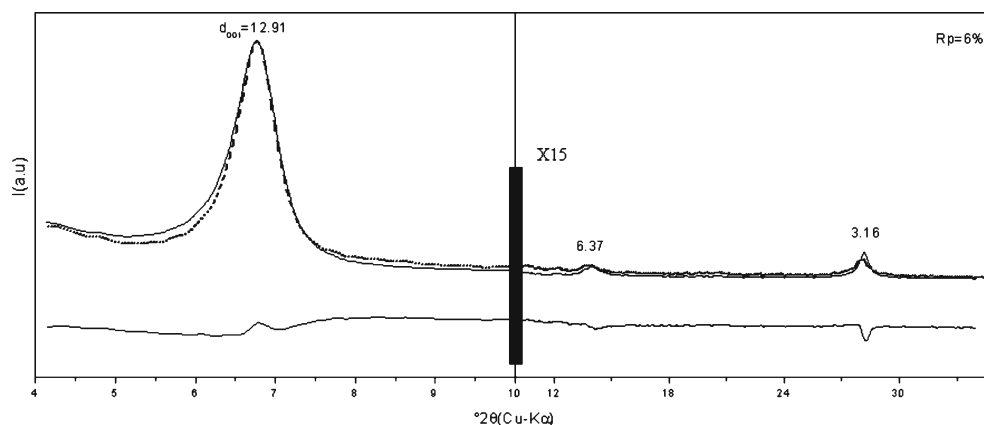


Figure 1. Experimental patterns of Ca-saponite recorded at different RH.

Table 1. Ca-saponite structural parameters deduced from XRD simulation ($n(\text{H}_2\text{O})$; number of water molecule; $Z(\text{H}_2\text{O})$; position of water molecule along c^* axis and W is abundance of water hydration state (per half unit cell)).

RH (%)		20–40	40–60	60–90
0W	d_{001}	10 Å	-	-
	W	0.12	-	-
	$n(\text{H}_2\text{O})$	-	-	-
	$Z(\text{H}_2\text{O})$	-	-	-
1W	d_{001}	12.6 Å	12.6 Å	-
	W	0.88	0.6	-
	$n(\text{H}_2\text{O})$	2.4	2.4	-
	$Z(\text{H}_2\text{O})$	9.4 Å	9.4 Å	-
2W	d_{001}	-	15.6 Å	15.6 Å
	W	-	0.4	0.83
	$n(\text{H}_2\text{O})$	-	3.2	3.2
	$Z(\text{H}_2\text{O})$	-	15.2–9 Å	15.2–9 Å
3W	d_{001}	-	-	18.6 Å
	W	-	-	0.17
	$n(\text{H}_2\text{O})$	-	-	4
	$Z(\text{H}_2\text{O})$	-	-	18–15–12 Å
Layer number		11	12	10
Succession law		Random	Random	Random

**Figure 2.** Best agreement between theoretical (—) and experimental (---) patterns of Ca-saponite at RH = 40%; (*) represents difference between theoretical and experimental patterns.

a total transition to 2 W state and vanishing of 1 W hydration state. For higher RH (80%), d_{001} appears at 16.11 Å indicating the presence of 3 W.

The quantitative study of XRD patterns allowed us to determine some structural parameters such as abundance, probabilities of each hydration state, number of layers, number and position of water molecules along the z axis. These parameters at different RH are shown in table 1.

Calculated and experimental profiles of Ca-saponite are shown as a function of relative humidity together with their difference plots in figures 2, 3.

Simulation of Ca-saponite XRD pattern (figure 2) shows that the best agreement between experimental and calculated

plots is obtained with R_p equal to 6% with 88% of 1 W and 12% of 2 W randomly distributed, the average number of layer is 11.

At high relative humidity, the interlayer space is characterized by the presence of 17% of 3 W and 83% of 2 W (figure 3) with reliability factor equal to 4%.

All structural parameters deduced from simulation are presented in table 1.

Comparing these results with those found for Ca-saponite with 0.4 charges per half unit cell (Karmous *et al* 2009), we can conclude that increasing layer charge leads to the formation of a more structured water and shifts hydration transitions toward lower relative humidity conditions.

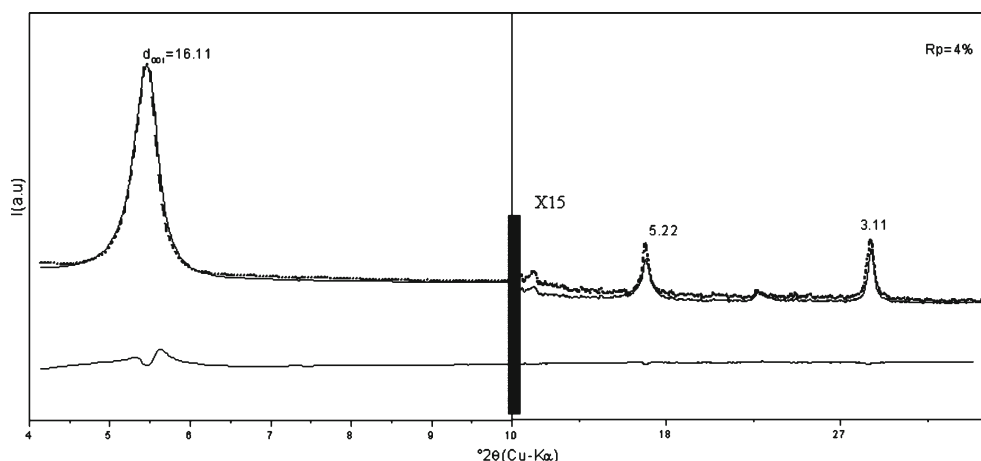


Figure 3. Best agreement between theoretical (—) and experimental (- - -) patterns of Ca-saponite at RH = 80%; (*) represents difference between theoretical and experimental patterns.

4. Conclusions

This study showed systematic hydration heterogeneity whatever the relative humidity (RH) and Ca-saponite sample presents many hydration states in whatever RH range. In all structural models the hydration states were randomly distributed in the interlayer space.

References

- Ben Haj Amara A, Ben Brahim J, Plançon A and Ben Rhaïem H 1998 *J. Appl. Crystallogr.* **31** 654
- Drits V A and Tchoubar C 1990 *X-ray diffraction by disordered lamellar structures: Theory and application to microdivided silicates and carbons* (New York: Springer)
- Ferrage E, Lanson B, Malikova N, Plançon A, Sakharov B A and Drits V A 2005a *Chem. Mater.* **17** 3499
- Ferrage E, Lanson B, Sakharov B A and Drits V A 2005b *Am. Mineral.* **90** 1358
- Ferrage E, Lanson B, Michot L J and Robert J L 2010 *J. Phys. Chem.* **C114** 4515
- Güven N 1988 *Hydrous phyllosilicates (exclusive of micas)* (ed.) S W Bailey (Washington D.C.: Mineralogical Society of America)
- Howard S A and Preston K D 1989 *Rev. Mineral.* **20** 217
- Karmous M S, Ben Rhaïem H, Naamen S, Oueslati W and Ben Haj Amara A 2006 *Z. Kristallogr. Suppl.* **23** 431
- Karmous M S, Oueslati W, Ben Rhaïem H, Robert J L and Ben Haj Amara A 2007 *Z. Kristallogr. Suppl.* **26** 503
- Karmous M S, Ben Rhaïem H, Robert J L, Lanson B and Ben Haj Amara A 2009 *Appl. Clay Sci.* **46** 34
- Laird D A 2006 *Appl. Clay Sci.* **34** 74
- Mooney R W, Keenan A G and Wood L A J 1952 *J. Am. Chem. Soc.* **74** 1371
- Pons C H, De la calle C and de Vidales M 1995 *Clays Clay Miner.* **43** 246